

# Introducing thermodiffusive effects in large-eddy simulation of turbulent combustion for lean hydrogen-air flames

By A. Aniello<sup>†</sup>, D. Laera<sup>‡</sup>, L. Berger<sup>¶</sup>, A. Attili<sup>||</sup> AND T. Poinsot<sup>†</sup>

Thermodiffusive instabilities induced by low-Lewis number effects can be triggered in premixed hydrogen-air mixtures, affecting both laminar and turbulent combustion. These effects are introduced in a formulation based on the thickened flame model by assuming that the characteristic lengths at which these instabilities occur are smaller than the wrinkling scales induced by turbulent eddies. This hypothesis allows us to build a combustion subgrid-scale model decoupling the enhancement of the burning rate due to (i) thermodiffusive instabilities and to (ii) usual turbulence wrinkling. Direct Numerical Simulation (DNS) of laminar lean atmospheric hydrogen-air flames (Berger *et al.* 2022*a,b*) are used to parameterize these subgrid scale effects introducing them into a compressible LES code. The updated numerical model is finally tested on swirling hydrogen-air flames experimentally investigated at Institut de Mécanique des Fluides de Toulouse (IMFT). The new model increases the local consumption rate in all premixed, lean flame zones and leaves the rich parts of the flame as well as the diffusion flame zones untouched. This is a first example of the practical implementation of thermodiffusive effects in a LES code utilizing the thickened-flame model.

---

## 1. Motivations and objectives

Understanding and predicting hydrogen-air flame structures are major challenges for all future engine applications as well as a classical problem in the combustion community (Schefer *et al.* 1994; Schefer & Goix 1998; Lipatnikov & Chomiak 2005; Su *et al.* 2006; Guiberti *et al.* 2019). The high reactivity of hydrogen and its great molecular diffusivity lead to radical differences compared to the combustion of usual hydrocarbons such as methane or kerosene, opening new challenges in the context of high-fidelity simulations. For example, in many applications, the high hydrogen reactivity allows the assumption that the characteristic chemical timescale is much smaller than the convective one, so that simplified modeling approaches can be used. For example, previous works exploited either strained diffusion flamelets (Pierce & Moin 2004; Pitsch 2006) or even infinitely fast chemistry assumption in the case of  $H_2/O_2$  flames (Urbano *et al.* 2016).

One specificity of lean hydrogen flames is their capacity to develop thermodiffusive instabilities (Matalon *et al.* 2003; Lipatnikov & Chomiak 2005) due to the disparity between molecular and thermal diffusions, which results in low-Lewis number effects.

<sup>†</sup> Institut de Mécanique des Fluides de Toulouse, 31057 Av. C. Soula, Toulouse, France

<sup>‡</sup> Centre Européen de Recherche et de Formation Avancée en Calculs Scientifique, 31400 Av. Coriolis, Toulouse Cedex, France

<sup>¶</sup> Institut für Technische Verbrennung, RWTH Aachen University, Germany

<sup>||</sup> Institute of Multiscale Fluids, University of Edinburgh, United Kingdom

When a propagating planar laminar flame is perturbed, the initial modification of the reaction layer is self-amplified, leading to the formation of cellular structures that modify the global flame characteristics (i.e., the integral burning rate) (Berger *et al.* 2022*a,b*; Howarth & Aspden 2022). Recent DNSs (Frouzakis *et al.* 2015; Berger *et al.* 2022*c*) have addressed the specificities of these instabilities in hydrogen-air flames, showing the capacities and the limits of the classical theories (Matalon *et al.* 2003). These studies confirmed that these cells and the straining effects induced by the low Lewis number of H and H<sub>2</sub> molecules create (i) a local modification of the consumption speed and (ii) an additional wrinkling of the flame front. These two effects have been extensively considered in the past for usual fuels characterized by Lewis number in the range of 0.7 to 3.0, and they are generally negligible. The consumption speed averaged along the flame front  $\langle s_c \rangle$  remains of the order of the laminar unstrained flame speed  $s_L^0$ , while the increase of flame surface due to these instabilities is negligible. Flame wrinkling in this situation, is mainly due to flame-turbulence interaction.

For hydrogen-lean flames, however, the situation is different. The DNS of Howarth & Aspden (2022) indicate that the ratio  $I_o = \langle s_c \rangle / s_L^0$  can reach values larger than 2. For turbulent flames, Berger *et al.* (2022*a,b,c*) suggest even a synergy between the turbulence wrinkling and the strong preferential diffusion of lean H<sub>2</sub> mixtures. They simulated a slot burner configuration with homogeneous turbulent injection and found the turbulent flame speed  $s_T$  in the case of thermodiffusive instabilities increases by more than a factor of 4 with respect to the case of unity Lewis number. These flames are shorter than normally expected and show local super-adiabaticity that may potentially lead to higher NOx emissions, which is a major concern of H<sub>2</sub> flames. Clearly, a turbulent combustion model for LES of hydrogen flames that aims at being representative of the flame shape and pollutant emissions must contain these effects. This is the main topic of the present study.

An additional complexity of hydrogen flames is created by the effects due to the increase of pressure. While most laboratory experiments are performed at 1 bar, real chambers operate from 15 to 50 bars. Under these conditions, all molecular diffusivity coefficients decrease ( $\approx 1/P$ ), the Reynolds number increases and the characteristic flame thickness decreases. As a consequence, a direct simulation of those operating conditions becomes prohibitive and reliable subgrid-scale combustion models must be adopted for flame-turbulence interaction. Of course, similar issues arise for kerosene or methane flames too, but for hydrogen, more complex dynamics are expected since pressure amplifies the impact of thermodiffusive instabilities. The stabilization mechanisms or thermo-acoustic responses of hydrogen flame at high pressure can be completely different than those at atmospheric conditions.

Another important aspect specific to hydrogen flames is that the impact of thermodiffusive instabilities depends on the combustion regime. Diffusion flames do not exhibit any intrinsic thermodiffusive instability, while lean premixed flames are highly susceptible to their effects. As a consequence, a fair evaluation of thermodiffusive phenomena requires a proper prediction of the dominant combustion regimes in the specific applications. This is particularly important for H<sub>2</sub> flames, since, in order to avoid safety issues (i.e., flashback or explosions in feeding lines) caused by their high reactivity, reactants are commonly injected separately, leading to a variety of potential stabilization and combustion regimes. Such flames can be anchored near the lip of the injection devices. In this first case, as a result of the long mechanical mixing times compared to chemical times associated with hydrogen chemistry, flames are mainly diffusion-controlled and thermodiffusive effects are

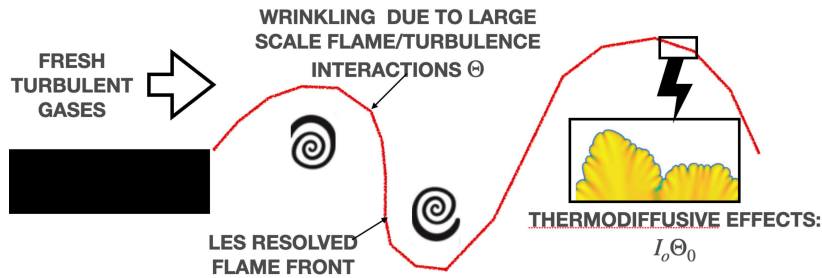


FIGURE 1. Scale separation principle of the TD-TFLES model for LES of turbulent hydrogen flames, including thermodiffusive effects.  $\Theta$  is the wrinkling induced by turbulence,  $\Theta_0$  is the wrinkling induced by thermodiffusive effects at subgrid scale and  $I_o$  measures the changes of the local consumption speed induced by thermodiffusive phenomena.

negligible. However, depending on the flow and the mixing devices implemented inside a hydrogen injection device, flames can also be lifted from the injection lips, a property that is useful to limit the thermal load on walls and the NO<sub>x</sub> emissions. In this second case, depending on the distance between the flame and the injector lips, various degrees of mixing between reactants are possible, and fronts propagating in lean zones may trigger thermodiffusive effects. Hence, LES combustion models for hydrogen must account not only for the thermodiffusive instabilities, but also modulate their influence depending on the combustion regime encountered. This aspect is specific to LES of real flames. Most DNS of hydrogen flames have been limited to perfectly premixed cases so that new additional physics is expected when going to real hydrogen combustors.

The present study proposes a first LES model, in the framework of the TFLES formulation (Colin *et al.* 2000), taking into account hydrogen thermodiffusive effects by introducing DNS correlations obtained by Berger *et al.* (2022*a,b*) to account for thermodiffusive effects. The initial model is called TFLES, while the new one is designated as TD-TFLES for thermodiffusive TFLES. The implementation and the limits of the proposed model are described in the next section. The TD-TFLES is then tested against experimental data gathered at IMFT on a swirled hydrogen-air turbulent flame and compared to the results previously obtained with the standard TFLES approach.

## 2. A DNS-based TFLES model incorporating thermodiffusive effects for hydrogen flames (TD-TFLES)

This study proposes to include the effect of thermodiffusive instabilities in LES combustion models based on the thickened flame formalism. Both flame-turbulence interaction and thermodiffusive instabilities generate flame surface wrinkling that can alter the local burning rate. Hence, these two mechanisms are expected to compete, or at least co-exist, in the same model. Note that this is somewhat new in the turbulent combustion community, which has been consistently ignoring thermodiffusive effects in turbulent flames for decades, despite theoretical and experimental evidence pointing out that this simplification was not always justified (Matalon *et al.* 2003; Lipatnikov & Chomiak 2005).

At this point, it is useful to introduce notations: following Howarth & Aspden (2022),  $I_o$  is the ratio of  $\langle s_c \rangle$  over  $s_L^0$ . The flame wrinkling induced by thermodiffusive effects will be designated as  $\Theta_0$  and the wrinkling induced by turbulence  $\Theta$ . As a basic assumption for the first form of the TD-TFLES model, we loosely imply that the wrinkling induced

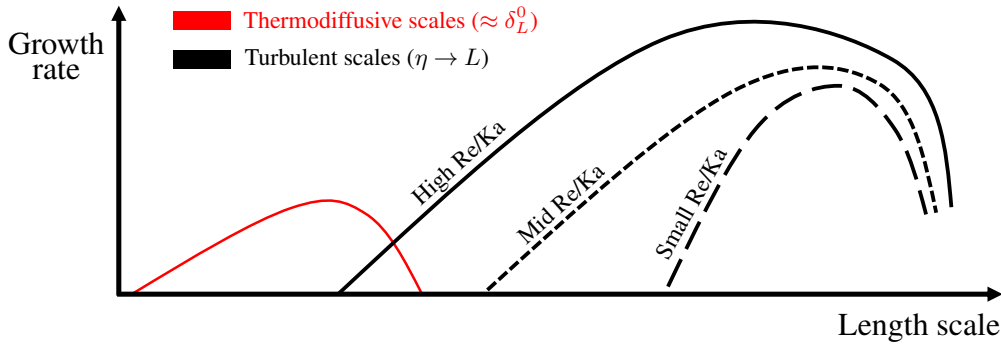


FIGURE 2. Representation of the scale-separation assumption between thermodiffusive wrinkling and turbulence wrinkling used in the TD-TFLES model.

by thermodiffusive effects ( $\Theta_0$ ) and by turbulence ( $\Theta$ ) are decoupled. Therefore, the starting point of the model consists in considering that the length scales of the cellular structures produced by thermodiffusive effects ( $\approx \delta_L^0$ ) are much smaller than the wrinkling scales induced by flame-turbulence interaction (Figure 1). These turbulent scales vary widely between the integral scale of the turbulence ( $L$ ) and the Kolmogorov scale ( $\eta$ ). In spectral space, this model works under the assumption of scale separations (Figure 2): Thermodiffusive instabilities act at small scales while turbulence scales are all larger.

Clearly, not all flames will satisfy the assumption used to build the TD-TFLES model. Consider a burner where typical integral scales, imposed by the geometry, are of order  $L$ . This size  $L$  for most burners of interest is much larger than the flame thickness  $\delta_L^0$ , so that the TD-TFLES idea works for them. However, the question is to know whether all other turbulent scales also fulfill the scale-separation assumption. The smallest one will be the Kolmogorov scale. For the TD-TFLES to work at all scales, the Kolmogorov scale should also be larger than the characteristic flame length  $\delta_L^0$ . This is verified for low Reynolds numbers, and in this case the Kolmogorov scale  $\eta$  will also be large compared to  $\delta_L^0$ , so that the TD-TFLES model idea can be applied (the Karlovitz number  $K_a = (\delta_L^0/\eta)^2$  will be low). When the flow rates and the Reynolds number increase, however, the Kolmogorov scale  $\eta$  will decrease and eventually reach the same order of magnitude as  $\delta_L^0$ , at which thermodiffusive instabilities occur. In this case, the TD-TFLES model should not be used. The small turbulence scales will interact with the thermodiffusive scales in a manner that is still open to speculations and these regimes are left for further research.

Under the TD-TFLES assumption, the turbulent flame speed  $s_T$  can then be expressed as

$$s_T = s_L^0 I_o \Theta_0 \Theta. \quad (2.1)$$

In this TD-TFLES approach, thermodiffusive effects are completely modeled as a subgrid-scale phenomena, since the spatial discretization provided by the LES solver is supposed to be too coarse to capture the thermodiffusive scales. Hence,  $I_o$  and  $\Theta_0$  are not resolved by the LES solver. However, the wrinkling  $\Theta$  due to turbulence-flame interaction, has a resolved part which is captured by the LES solver and a subgrid part which is modeled through the efficiency function of the TFLES model, as is usually done (Colin *et al.* 2000).

Furthermore, it must be emphasized that the present model can be regarded as a pure extension of the classical TFLES: fuels that do not exhibit TD instabilities will simply

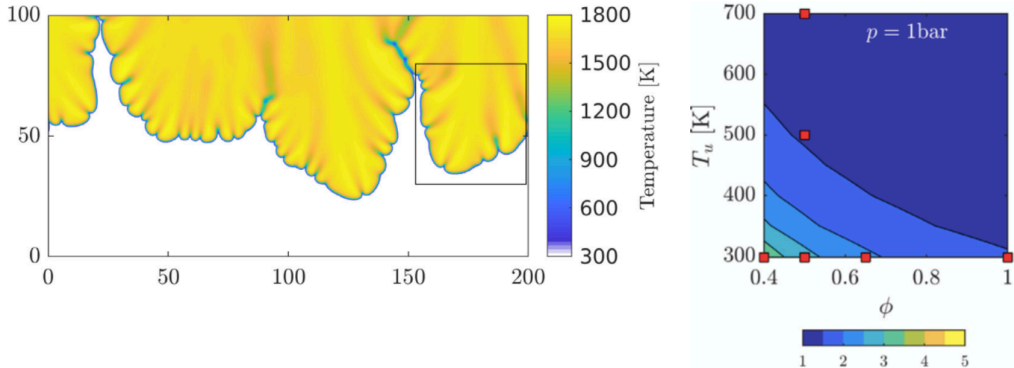


FIGURE 3. (Left) DNS of hydrogen-air laminar flames at equivalence ratio  $\phi = 0.4$  exhibiting thermodiffusive effects in hydrogen flames (Berger *et al.* 2022b). (Right) extracted values for  $I_o\Theta_0$  depending on  $P$ ,  $T$  and  $\phi$  used for the TD-TFLES implementation at 1 bar.

work under the assumption  $I_o = 1$  and  $\Theta_0 = 1$ , retrieving the standard modeling. In the general case, instead, the closure of the new LES model requires models for the two terms  $I_o$  and  $\Theta_0$ . Here this closure was obtained using the correlations of Berger *et al.* (2022a,b) extracted from DNS of lean hydrogen-air flames. In these DNSs, the overall speed of a laminar flame developing self-excited thermodiffusive instabilities was measured in a range of pressure  $P$  from 1 bar to 20 bar, fresh gas temperatures  $T_{fresh}$  ranging from 300 K to 700 K and a large range of equivalence ratios  $\phi$ . These thermodynamic conditions are representative of several combustion chambers targeted for real applications. A typical snapshot of such DNS throughout the non-linear regime is given in Figure 3 (left), which shows the temperature field of a premixed hydrogen-air flame at  $\phi = 0.4$  subjected to thermodiffusive instabilities. The flame front, initially flat, increases its surface and produces a self-sustained wrinkling due to low-Lewis number effects as well as a non-uniform wake of burnt gas temperature behind the flame front. Figure 3 (right) shows the resulting form for the correction  $I_o\Theta_0$  as a function of  $T_{fresh}$  and  $P$  and  $\phi$ :  $I_o\Theta_0$  tends to unity for near-stoichiometric or rich flames, while at atmospheric pressure, it can go up to 4 for very lean conditions ( $\phi < 0.4$ ). These correlations for  $I_o\Theta_0$  are tabulated and implemented in the LES model.

In the specific case of the swirling flame tested here,  $T_{fresh}$  and  $P$  are fixed to the inlet temperature of reactants and to the operating pressure of the combustion chamber, respectively. Because of a potential separated injection (as in this study), only the equivalence ratio variation must be considered locally and at each time step to retrieve the correct instantaneous efficiency value. The model can be extended to other systems characterized by temperature and pressure variations during the combustion processes (piston engines for example), informing the model for the thermodiffusive effects of the instantaneous and local thermodynamic conditions.

Once the increase of chemical reaction due to thermodiffusive effects  $I_o\Theta_0$  is known, it is implemented into the TD-TFLES model for combustion by multiplying both the diffusion term and the combustion term by  $I_o\Theta_0$ , exactly as is done for the efficiency function of the original TFLES model (Poinot & Veynante 2012). The influence of thermodiffusive instabilities must be eliminated for diffusion flame. This is done by evaluating the Takeno index (Yamashita *et al.* 1996) in space and time to distinguish between premixed or diffusion regimes and conditioning the application of the TD-TFLES accordingly.

Case	$\dot{m}_{air}$ [g/s]	$\dot{m}_{H_2}$ [g/s]	$U_b^{air}$ [m/s]	$U_b^{H_2}$ [m/s]	$P_{th}$ [kW]	$\phi_g$
<i>A</i>	2.41	0.032	11.4	13.6	3.89	0.45
<i>L</i>	6.03	0.080	28.5	34.0	9.73	0.45

TABLE 1. Mass flow rates of air and hydrogen, nominal thermal power  $P_{th}$  and global equivalence ratio  $\phi_g$  adopted for the two operating conditions *A* (attached flame) and *L* (lifted flame).

### 3. Application of the TD-TFLES models to a swirled hydrogen-air chamber

The TD-TFLES formulation was tested on the HYLON swirled hydrogen - air turbulent burner initially developed at EM2C in Centralesupelec (Figure 4) in a different framework (Degenève *et al.* 2019, 2021) and adapted to hydrogen during the ERC advanced grant SCIROCCO (cerfacs.fr/scirocco) at IMFT. Multiple diagnostics are available for this system and can be compared to LES data.

The HYLON burner was designed to stabilize hydrogen-air swirled flames and can produce different flame archetypes. In the inlet section of the burner, turbulent mixing induced by the turbulent flow competes with the chemical times of hydrogen-air chemistry, and the outcome of this competition leads to either an anchored flame or a lifted one. The transition between the two is controlled by the aerodynamic field imposed at the injector outlet and by both hydrogen and air flow rates (Table 1). The first are attached to the lips of the injection system and are completely diffusion-controlled. The latter has the potential of creating intense mixing before combustion, and a large portion of the flame burns in premixed conditions (case L in Figure 4).

The simulation tool is the compressible solver AVBP (Gourdain *et al.* 2009; Poinso 2017) in which flame-turbulence interactions are modeled using the TFLES model (Colin *et al.* 2000; Kuenne *et al.* 2011; Wang *et al.* 2011). The grid counts 58 M tetrahedral cells, with a minimum characteristic size of 100  $\mu\text{m}$  in the flame stabilization region. The mesh size distribution varies between 100  $\mu\text{m}$  and 200  $\mu\text{m}$  along the two coaxial injectors to capture the strong radial velocity gradients of the hydrogen flow and retrieve the correct velocity field. Heat losses through the walls are modeled for the two flames by imposing the external wall temperature given by experiments and a local heat resistance. For the combustion chamber walls, a constant thermal resistance  $R = 0.004 \text{ W/m}^2\text{K}$  is imposed considering the thickness of the quartz windows to be  $l_q = 8 \text{ mm}$  and a thermal conductivity of  $\lambda_q = 2.07 \text{ W/mK}$ . Inlet mass flow rates and outlet pressure are imposed using the NSCBC approach (Poinso *et al.* 1992). The chemistry description relies on a semi-detailed San Diego chemical mechanism (Saxena *et al.* 2006) that comprises 9 transported species and 21 reactions.

The effects of the model are assessed by comparing the standard TFLES and TD-TFLES for the lifted flame *L*, which corresponds to the case of practical interest. Both simulations using TFLES and TD-TFLES were run for 25 ms corresponding to two flow-through times at the bulk velocity that was found sufficient to reach steady state and gather statistics. For this flame, Table 2 summarizes numerical and physical parameters used in the LES.

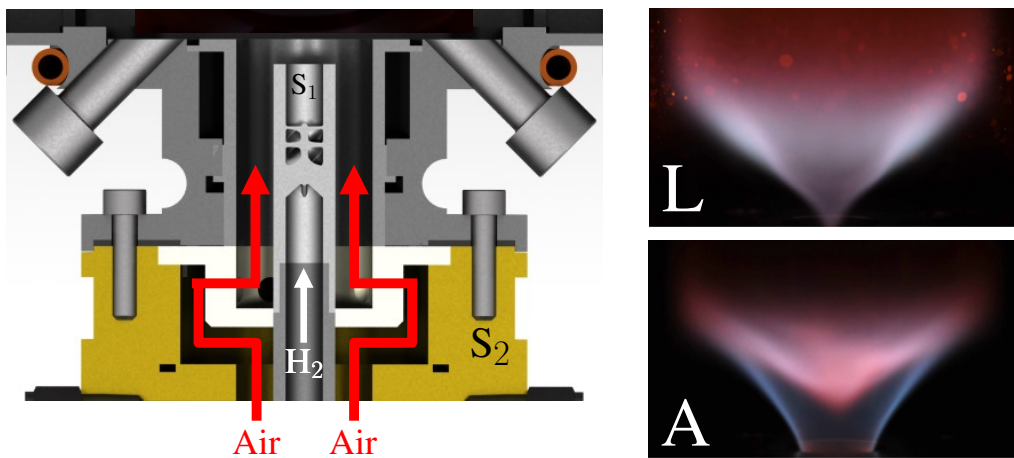


FIGURE 4. The HYLON dual-swirl burner for hydrogen-air combustion. (Left) Schematic of the injection system with annular injection of air and central injection of hydrogen stream.  $S_1$  and  $S_2$  denote the internal and external swirlers of the coaxial injectors. (Right) Line of sight integrated images for lifted (top) and attached (bottom) flames. Source: H. Magnes, S. Marragou & T. Schuller, IMFT.

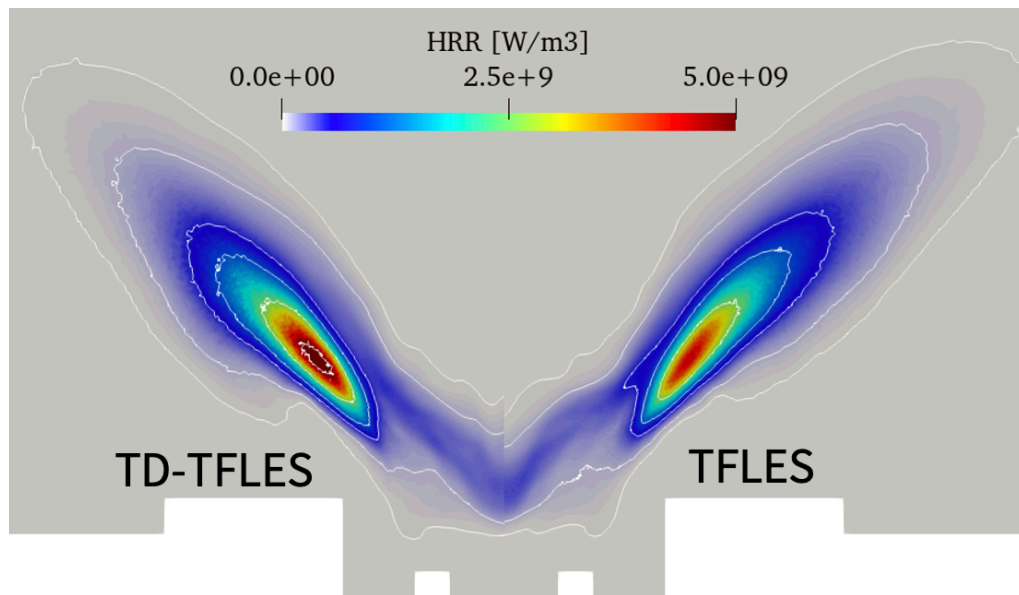


FIGURE 5. Cut in the central plane of the experiment for flame  $L$ . Mean fields of heat release rate for TD-TFLES (left) and TFLES (right).

Since the injection lines of hydrogen and air in HYLON are separated, a wide range of equivalence ratios is expected in the chamber zone where combustion takes place, so that the  $I_o\Theta_0$  correction of Figure 3 should be active on the premixed lean side of the flame in multiple places.

The first overall result is that the introduction of the TD model does not change the

Total mesh cells	$\approx 51$ M Unstructured
Convection scheme	Lax Wendroff
CFL	0.7
Time step [s]	$9.0e-9$
Chemical scheme	San Diego (ARC 9s21r)

TABLE 2. Numerical setup characteristics in terms of mesh size, convection and chemical schemes.

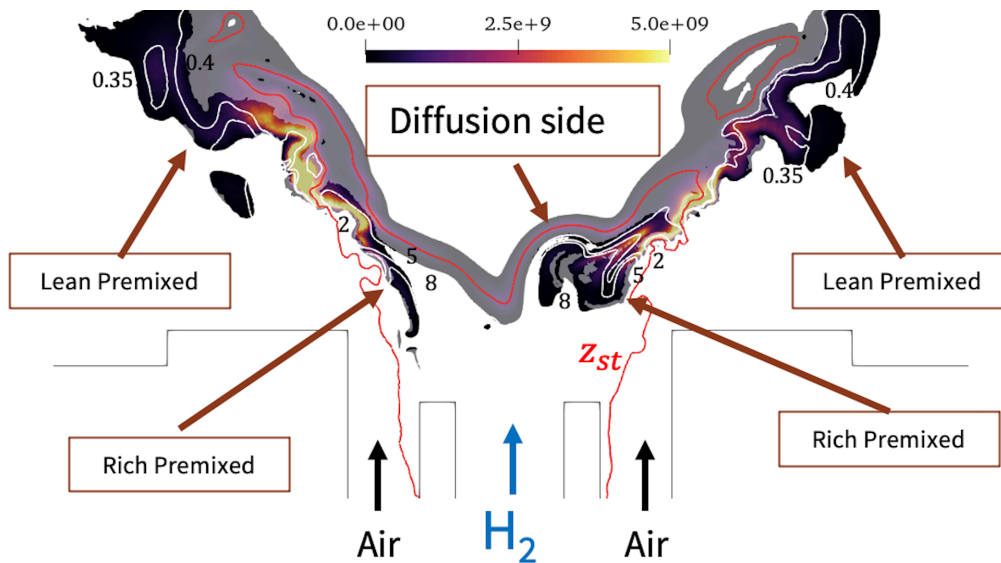


FIGURE 6. Cut in the central plane of the experiment for flame L. Instantaneous field of heat release rate for TD-TFLES. The red line represents the stoichiometric line  $z = z_{st}$ . The labels and the white lines correspond to local values of the equivalence ratio  $\phi$  computed using the definition of Bilger for the mixture fraction  $z$ .

flame position or behavior radically with respect to the previous formulation. Figure 5 shows the time-averaged fields of the reaction rates for the standard TFLES (right) and the TD-TFLES (left) over an axial plane of the combustor. Even if the TD-TFLES increases the local mean combustion intensity, the flame remains constrained by the recirculation zone and does not change its position significantly, as shown by an instantaneous field of heat release rate in Figure 6, which also shows the lifted nature of the flame.

First, the lower sides of the flame wings are characterized by premixed combustion: hydrogen and air mix at the injector mouth before burning in premixed mode. Above the injector lips of the combustor (inside the  $z = z_{st}$  line), the mixture is very rich ( $2 < \phi < 8$ ), since the supply of reactants in this zone is mainly due to the central injection. Further downstream along the flame wings, the longer mixing time allowed between hydrogen and air leads to leaner flames ( $\phi < 0.5$ ). On the combustor axis,

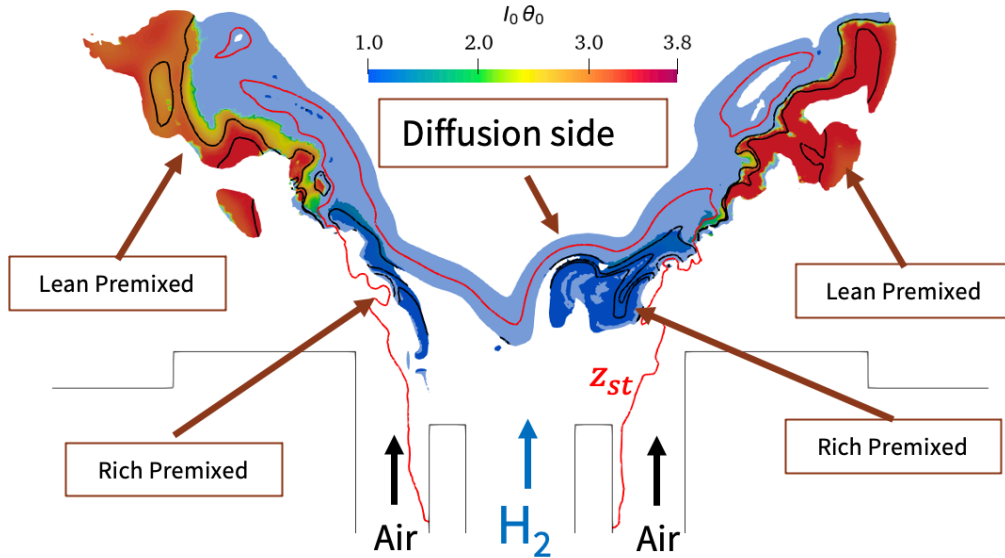


FIGURE 7. Cut in the central plane of the experiment for flame  $L$ . Fields of the thermodiffusive efficiency  $I_0\Theta_0$  for TD-TFLES conditioned on the flame location. The red line represents the stoichiometric line  $z_{st}$ .

a diffusion flame is formed between the hydrogen central stream and the equilibrium products (still rich in  $O_2$ ) recirculating in the inner recirculation zone.

As expected, the  $I_0\Theta_0$  correction introduced in the TD-TFLES model does not modify the diffusion flame zones or the rich premixed flamelets. The field of  $I_0\Theta_0$  (Figure 7) shows that the model leads to  $I_0\Theta_0$  values different from unity (unity corresponding to no effect) only in the lean premixed flames at the flame tip, increasing the local reaction rate by factors up to 4 in the very lean zones. The model is also inactive in the zones where mixing takes place, close to the  $H_2$  injector.

#### 4. Conclusions

A model for thermodiffusive instabilities for lean hydrogen-air flames was added in the classical TFLES formalism, assuming scale separation between the (small) thermodiffusive scales and the (large) turbulent scales. This additional model requires closure laws for two effects: (i) subgrid-scale wrinkling ( $\Theta_0$ ) due to cell formations and (ii) modification of the mean consumption rate ( $I_0$ ). Both were obtained from the DNS of self-excited atmospheric hydrogen-air flames by Berger *et al.* (2022b).

The DNS correlations were introduced in the LES AVBP code as a tabulation and used as an additional efficiency function to increase the local reaction rates accordingly.

The LES solver was run for the swirler hydrogen-air chamber developed by IMFT. Results show that thermodiffusive instabilities increase local reaction rates by a significant factor in the lean parts of the flame ( $\phi < 0.4$ ) but leave the diffusion flame zones as well as the rich premixed flamelets unaffected.

In the case of the IMFT chamber studied here, the modified TD-TFLES model leads to an increase of local reaction rates, but the flame position, which is fixed mainly by the flow, is marginally affected because the lean premixed regions are limited and the flame is dominated by a large diffusion zone as well as premixed rich zones.

Future work will be needed to test the model on other flames and improve it to relax the scale separation assumptions used to build it. The effects of the model on  $\text{NO}_x$  emissions will also be evaluated.

## Acknowledgments

The support of Dr. E. Riber and Dr. O. Vermorel (CERFACS) in the development of the AVBP version used here is gratefully acknowledged as well as the help of S. Marragou, H. Magnes and Prof. T. Schuller in providing CAD data, operating regimes and experimental results for the HYLON burner of IMFT. The interactions with CTR hosts J. Wang and K. Maeda and with Prof. H. Pitsch and P. Moin were especially fruitful.

## REFERENCES

- BERGER, L., ATTILI, A. & PITSCH, H. 2022a Intrinsic instabilities in premixed hydrogen flames: Parametric variation of pressure, equivalence ratio, and temperature. Part 1 - Dispersion relations in the linear regime. *Combust. Flame* p. 111935.
- BERGER, L., ATTILI, A. & PITSCH, H. 2022b Intrinsic instabilities in premixed hydrogen flames: parametric variation of pressure, equivalence ratio, and temperature. part 2 – non-linear regime and flame speed enhancement. *Combust. Flame* p. 111936.
- BERGER, L., ATTILI, A. & PITSCH, H. 2022c Synergistic interactions of thermodiffusive instabilities and turbulence in lean hydrogen flames. *Combustion and Flame* **244**, 112254.
- COLIN, O., DUCROS, F., VEYNANTE, D. & POINSOT, T. 2000 A thickened flame model for large eddy simulations of turbulent premixed combustion. *Phys. Fluids* **12** (7), 1843–1863.
- DEGENÈVE, A., MIRAT, C., CAUDAL, J., VICQUELIN, R. & SCHULLER, T. 2019 Effects of swirl on the stabilization of non-premixed oxygen enriched flames above coaxial injectors. *J. Eng. Gas Turb. Power* **141**, 121018.
- DEGENÈVE, A., VICQUELIN, R., MIRAT, C., CAUDAL, J. & SCHULLER, T. 2021 Impact of co- and counter-swirl on flow recirculation and liftoff of non-premixed oxy-flames above coaxial injectors. *Proc. Combust. Inst.* **38**, 5501–5508.
- FROUZAKIS, C. E., FOGLA, N., TOMBOULIDES, A. G., ALTANTZIS, C. & MATALON, M. 2015 Numerical study of unstable hydrogen/air flames: Shape and propagation speed. *Proc. Combust. Inst.* **35** (1), 1087–1095.
- GOURDAIN, N., GICQUEL, L., MONTAGNAC, M., VERMOREL, O., GAZAIX, M., STAFFELBACH, G., GARCIA, M., BOUSSUGE, J. & POINSOT, T. 2009 High performance parallel computing of flows in complex geometries: I. methods. *Comput. Sci. Disc.* **2**, 015003.
- GUIBERTI, T., BOYETTE, W., MASRI, A. & ROBERTS, W. 2019 Detachment mechanisms of turbulent non-premixed jet flames at atmospheric and elevated pressures. *Combust. Flame* **202**, 219–227.
- HOWARTH, T. & ASPDEN, A. 2022 An empirical characteristic scaling model for freely-propagating lean premixed hydrogen flames. *Combust. Flame* **237**, 111805.
- KUENNE, G., KETELHEUN, A. & JANICKA, J. 2011 LES modeling of premixed combustion using a thickened flame approach coupled with FGM tabulated chemistry. *Combust. Flame* **158** (9), 1750 – 1767.

- LIPATNIKOV, A. & CHOMIAK, J. 2005 Molecular transport effects on turbulent flame propagation and structure. *Progress in Energy and Combustion Science* **31** (1), 1–73.
- MATALON, M., CUI, C. & BECHTOLD, J. K. 2003 Hydrodynamic theory of premixed flames: effects of stoichiometry, variable transport coefficients and arbitrary reaction orders. *J. Fluid Mech.* **487**, 179–210.
- PIERCE, C. D. & MOIN, P. 2004 Progress-variable approach for large eddy simulation of non-premixed turbulent combustion. *J. Fluid Mech.* **504**, 73–97.
- PITSCH, H. 2006 Large eddy simulation of turbulent combustion. *Annu. Rev. Fluid Mech.* **38**, 453–482.
- POINSOT, T. 2017 Prediction and control of combustion instabilities in real engines (Invited Hottel lecture). *Proc. Combust. Inst.* pp. 1–28.
- POINSOT, T., ECHEKKI, T. & MUNGAL, M. G. 1992 A study of the laminar flame tip and implications for premixed turbulent combustion. *Theoretical and Numerical Combustion* **81** (1-3), 45–73.
- POINSOT, T. & VEYNANTE, D. 2012 *Theoretical and Numerical Combustion*, 3rd ed. Amazon.
- SAXENA, P. & WILLIAMS, F. 2006 Testing a small detailed chemical-kinetic mechanism for the combustion of hydrogen and carbon monoxide. *Combust. Flame* **145**, 316–323
- SCHEFER, R. W. & GOIX, P. 1998 Mechanisms of flame stabilization in turbulent lifted-jet flames. *Combust. Flame* **112**, 559–570.
- SCHEFER, R. W., NAMAZIAN, M. & KELLY, J. 1994 Stabilization of lifted turbulent-jet flames. *Combust. Flame* **99**, 75–86.
- SU, L., SUN, O. & MUNGAL, M. 2006 Experimental investigation of stabilization mechanisms in turbulent, lifted jet diffusion flames. *Combust. Flame* **144**, 494–512.
- URBANO, A., SELLE, L., STAFFELBACH, G., CUENOT, B., SCHMITT, T., DUCRUIX, S. & CANDEL, S. 2016 Exploration of combustion instability triggering using Large Eddy Simulation of a multiple injector liquid rocket engine. *Combust. Flame* **169**, 1–12.
- WANG, G., BOILEAU, M. & VEYNANTE, D. 2011 Implementation of a dynamic thickened flame model for large eddy simulations of turbulent premixed combustion. *Combust. Flame* **158** (11), 2199 – 2213.
- YAMASHITA, H., SHIMADA, M. & TAKENO, T. 1996 A numerical study on flame stability at the transition point of jet diffusion flame. In *26th Symp. (Int.) on Combustion*, pp. 27 – 34. The Combustion Institute, Pittsburgh.